PHYSICAL REVIEW A VOLUME 20, NUMBER 3 SEPTEMBER 1979

Collective ordering phenomena and instabilities of the ^{27}Al nuclear spin system in ruby

P. Bösiger, E. Brun, and D. Meier
Physik-Institut, Universität Zürich, Zürich, Switzerland
(Received 20 February 1979)

The dynamic properties of the ruby NMR laser are discussed from the point of view of synergetics. The authors present a theoretical approach together with the experimental verification. The cooperative features of the instabilities and the disorder-order transitions far from thermal equilibrium of the ruby NMR laser are described by means of order parameters and their dynamic equations, which are generalized Bloch equations. The heat-reservoir description of the conventional spin dynamics in ruby is thereby taken into account. The theory is applied to the free-running NMR laser with its threshold, the critical narrowing of cw NMR lines below threshold, and the steady-state output above threshold. The theory is then extended to the driven NMR laser where an external resonant rf field is applied to form, together with the self-induced radiation field, a competitive- or cooperative-field configuration. The authors present data concerning bistability and hysteresis of the driven NMR laser; in particular, its first-order-type phase transitions from a competitive- to a cooperative-field configuration are discussed. Finally, a novel pulsation mode of the ruby NMR laser is described.

I. INTRODUCTION

In systems composed of a great number of distinct entities (electrons, atoms, molecules, nuclear and electronic spins, living cells, persons, etc.) which are put under defined physical constraints, there may exist an interaction of cooperative nature which, on a macroscopic scale, can lead to a collective behavior of the individuals such that the whole is more than the mere addition of its parts. In particular, highly organized spatial and/or temporal structures may develop out of chaotic states; the system thus is undergoing a disorder-order transition. Such phenomena are found in a great variety of disciplines ranging from pure and applied physics over chemistry and biology to sociology, and are subject of the rapidly growing interdisciplinary field "Synergetics," as it is called by its founder H. Haken.[1] The most fascinating aspect of these phenomena is the apparent similarity and correspondence of the various disorder-order transitions even though the specific systems differ widely in composition and character of their constituents as well as on the macroscopic boundary conditions (open, closed, equilibrium, nonequilibrium, etc.). For example, prototypes of open systems far from thermal equilibrium are the laser-type devices. After the technical realization of the spin-flip ruby NMR laser[2] as a coherent source of radio frequency waves, we investigated in particular the cooperative features of the disorder-order transition to a superradiant state of this open system. Hence, we searched for a description of the macroscopic behavior by means of order parameters with their abrupt or continuous changes when certain physical variables (constraints) are varied. In a recent publication[3] we discussed a Bloch-type approach to the problem of nuclear superradiance which has its roots in the effects of radiation damping on spin dynamics.[4–7] In particular, we described the nonequilibrium second-order type phase transition from an incoherently to a coherently radiating spin state using a Landau-type dynamic order parameter equation for the rotating transverse nuclear magnetization M_γ. It became evident that such a nuclear spin system has specific properties making it suitable as an instructive example of synergetics. First, the time of evolution from one significant macroscopic state to another lies within an experimentally convenient time scale (microseconds to seconds). Second, a simple and reasonable theoretical approach to the different questions is available. Third, all the decisive physical quantities, which determine the macroscopic dynamics, can be measured or estimated with a high degree of accuracy. The purpose of this paper, which is an extension of the earlier work,[3] is to report in detail on the ruby NMR laser from the view point of synergetics. However, it is not our intention to augment the many examples of synergetic behavior by just another one. What we wish to present is a model system for which a quantitative analysis is possible. We include in our discussion not only the free-running single-mode NMR laser but also the novel rf-driven NMR laser[8,9] which has features in common with a nonlinear system showing optical bistability and hysteresis.[10–13] In principle, we have the NMR analogue of optically bistable devices, which

have caused much excitement lately in quantum optics. Here we treat the case where an external rf field interacts with a nuclear spin system which is in or close to a superradiant state.

In Sec. II we give a summary of the experimental aspects of the ruby NMR laser and present experimental results concerning the NMR laser frequency, its stability, and pulling, on which the theoretical model is based.

In Sec. III we describe the spontaneous second-order type phase transition from a disordered to an ordered superradiant single-mode spin state near threshold. We then compare theory and experiment which concern the NMR laser output and the critical narrowing of steady state NMR lines near the bifurcation point. For this free-running NMR laser the rotating field B_1, which slaves the nuclear spins, consists of the self-induced field B_1^{ind} and a fluctuating field $F_B(t)$. B_1^{ind} is the result of the phase-locked precession of the spins in a static magnetic field; $F_B(t)$ is due to the thermal noise current in the NMR coil. In Sec. IV we extend our considerations to the driven single mode NMR laser, where an external rf field B_1^{ex} is superimposed on B_1^{ind} and $F_B(t)$. Drastic reaction effects occur when the frequency of B_1^{ex} is close to the laser frequency. Since the response is exceedingly complicated in general, we restrict ourself to a situation where this field is in exact resonance such that B_1^{ex} and B_1^{ind} are either parallel ($B_1^{\mathrm{ex}}\uparrow\uparrow B_1^{\mathrm{ind}}$) or antiparallel ($B_1^{\mathrm{ex}}\uparrow\downarrow B_1^{\mathrm{ind}}$). In the former case we speak of a cooperative configuration, in the latter of a competitive one. Under the joint action of B_1^{ex}, B_1^{ind}, and $F_B(t)$ the nuclear spin order shows instabilities which lead to first-order-type phase transitions with their well-known bistability and hysteresis effects.

II. RUBY NMR LASER: EXPERIMENTAL ASPECTS

At liquid He temperature and in a strong magnetic field, self-induced collective rf oscillations of the ^{27}Al nuclear spins in Al_2O_3:Cr^{3+} can be observed when the spin population is inverted and the sample is placed in a laser-type feedback system, here an LC circuit, to produce stimulated spin flips. The laser action can easily be detected by an oscilloscope directly connected to the resonant circuit which is tuned to one of the quadrupolar split ^{27}Al NMR lines, while powerful microwave radiation is supplied to the sample in the vicinity of a selected Cr^{3+} ESR line. The microwave source (~100 mW) acts as a pump causing the population inversion over the nuclear Zeeman states by dynamic nuclear polarization (DNP). The nuclear spin system is thus brought to a negative spin temperature θ_{Al} (~mK) and an enhanced negative, longitudinal nuclear magnetization M_z is formed. In terms of synergetics, DNP produces an enhanced longitudinal Zeeman order with M_z as the order parameter. The coil of the LC circuit provides the rotating radiation field B_1 which causes the phase-locked spin precession. Due to the coherent slaving of the individual ^{27}Al spins, a rotating component M_v of the nuclear magnetization is induced. Again in the language of synergetics, we speak of a superradiant or transverse spin order with M_v as the order parameter. Thus when superradiance occurs, longitudinal Zeeman order is continually transformed into transverse order.

Single-mode laser action can be obtained with a low-Q LC circuit. For example, if a circuit with $Q=60$ and a filling factor of $\eta\cong 0.6$ is tuned to the center of the $(\frac{1}{2},-\frac{1}{2})$ NMR transition, the NMR laser frequency ω is, within our present accuracy of 1 part in 10^5, equal to the NMR frequency ω_0 of the conventional central line, independent of pumping power or NMR laser output as indicated in Fig. 1. Since the result reflects the modest stability of our magnet, a much better agreement can be anticipated for highly stabilized magnetic fields. The NMR laser frequency can be pulled by detuning the LC circuit to a frequency ω_c as it is shown in Fig. 2. The pulling can be calculated from the formula $\omega=(\omega_c/T_2+\omega_0/T_c)/(1/T_2+1/T_c)$[14,15] with T_2 the transverse nuclear relaxation time and T_c the ringing time of the circuit.

For what follows, we always assume perfect tuning of the LC circuit (and of a driving field, if present) to a selected NMR line. Such a system

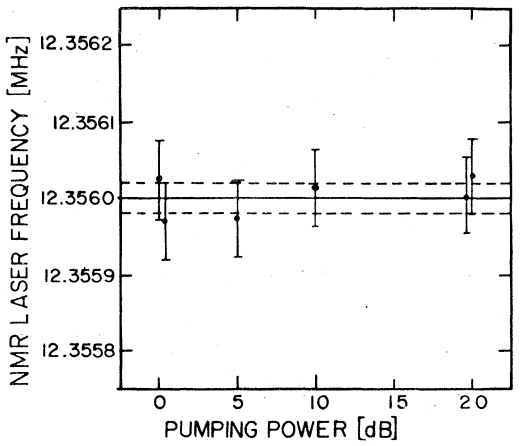

FIG. 1. NMR laser frequency as a function of the pumping power. The frequency is independent of the pumping power as predicted by the theory, if the tuning frequency of the LC circuit is equal to the Larmor frequency of the nuclear spins.

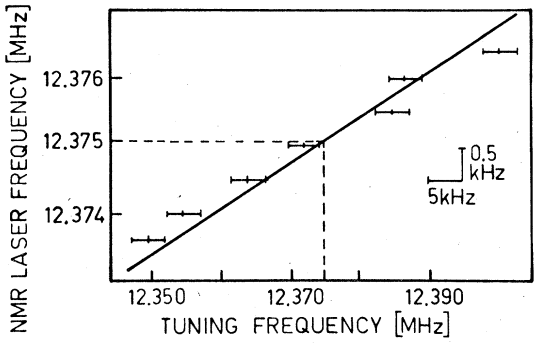

FIG. 2. NMR laser frequency pulling by detuning the LC circuit. The theoretical dependence (solid line) is determined by $\omega = (\omega_c/T_2 + \omega_0 T/_c)/({}^1/T_2 + {}^1/T_c)$. The dashed lines indicate perfect tuning $\omega = \omega_0 = \omega_c$.

then reacts purely absorptive. Hence, in a frame of reference rotating at the NMR frequency, the system can be described by the three macroscopic variables M_z, M_v, and B_1 where the subscript v stems from the well-known v or absorption mode.[16] Under such circumstances, Bloch-type equations are expected to describe the dynamics of the solid state NMR laser with reasonable accuracy. This has been experimentally proved in our previous work.[3] However, if the NMR laser is pulled out of resonance, dispersive effects are expected to show up which, presumably, will need a more refined treatment. It is well known that the saturation of the dispersive u mode in solids cannot be handled by simple Bloch equations as has been shown by Redfield[17] and this will possibly be true also for the highly nonlinear NMR laser.

III. FREE-RUNNING NMR LASER

If the ruby crystal is oriented such that a fully resolved quadrupole structure of its five $\Delta m = \pm 1$ NMR transitions can be observed, and the LC circuit is tuned to the central $(\frac{1}{2}, -\frac{1}{2})$ line, then the superradiant ^{27}Al spins $(I = \frac{5}{2})$ form a fictitious spin-$\frac{1}{2}$ two-state system. The NMR laser variables fulfill the equations

$$\dot{M}_v = 9\gamma M_z B_1 - M_v/T_2 , \tag{1a}$$

$$\dot{M}_z = -\gamma M_v B_1 - (M_z - M_e)/T_e , \tag{1b}$$

$$B_1 = B_1^{\mathrm{ind}} + F_B(t) . \tag{1c}$$

Here, γ is the gyromagnetic ratio, T_2 the dephasing or transverse relaxation time, T_e the effective pumping time, and M_e the pumping magnetization. T_e and M_e are parameters which can be derived from the extended heat reservoir model of DNP in ruby.[3] Note that T_e (~0.15 s) is much shorter than the spin-lattice relaxation time T_1 (~240 s), but long compared to T_2 (~3×10^{-5} s). With $Q = 60$ and $\omega_0 \cong 2\pi \times 12$ MHz, the LC circuit has an unloaded ringing time $T_c \cong 10^{-6}$ s, which is by far the shortest time constant in the system. Thus B_1^{ind} responds promptly to M_v such that

$$B_1^{\mathrm{ind}} = -\tfrac{1}{2}\mu_0 \eta Q M_v . \tag{2}$$

Discarding the fluctuations for the time being, we can eliminate B_1 in (1a) and (1b) and obtain

$$\dot{M}_v = -\tfrac{9}{2}\mu_0 \eta Q\gamma M_z M_v - M_v/T_2 , \tag{3a}$$

$$\dot{M}_z = \tfrac{1}{2}\mu_0 \eta Q\gamma M_v^2 - (M_z - M_e)/T_e . \tag{3b}$$

Possible steady-state solutions are $M_z^s = M_e$ and $M_v^s = 0$, of which M_z^s is stable. To study the stability of M_v^s, we define as threshold pumping magnetization the negative quantity

$$M_e^{\mathrm{th}} = -2/9\mu_0 \eta Q\gamma T_2 . \tag{4}$$

For $M_e > M_e^{\mathrm{th}}$, $M_v^s = 0$ is stable. If the NMR laser is pumped below the threshold value, a transition to a new stable state $M_v^s \neq 0$ may be induced by the fluctuations $F_B(t)$. If M_z is close to M_e, we can neglect $\dot{M}_z$ in (3b). Thus M_z can be eliminated, and we end up with the single Landau-type order-parameter equation

$$\dot{M}_v = -\alpha M_v - \epsilon M_v^3 + \tilde{F}_B(t) , \tag{5a}$$

with

$$\alpha = 1/T_2 + \tfrac{9}{2}\mu_0 \eta Q\gamma M_e , \tag{5b}$$

$$\epsilon = (9/4)\mu_0^2 \eta^2 Q^2 \gamma^2 T_e . \tag{5c}$$

With increasing pumping power, α passes from positive to negative values. At $\alpha = 0$, the system reaches a critical point.

In weakly pumped states $\alpha > 0$ can be interpreted as an inverse effective dephasing time

$$1/T_{2\mathrm{eff}} = 1/T_2 + \tfrac{9}{2}\mu_0 \eta M_e . \tag{6}$$

Hence, $1/T_{2\mathrm{eff}}$ determines the cw linewidth of conventional NMR if saturation is avoided. With growing pumping power but keeping $\alpha > 0$, the system remains in a noncoherent radiation state but becomes more and more undamped. Under these circumstances the NMR lines of ruby narrow and grow critically. Since the five quadrupolar split NMR lines have different critical values for α, they differ in their enhancements as demonstrated in Fig. 3.

In the superradiant state ($\alpha < 0$) we find the stationary rotating nuclear magnetization

$$M_v^s = \frac{2}{3T_2\mu_0 \eta Q\gamma}\left[\left(\frac{T_2}{T_e}\right)\frac{M_e - M_e^{\mathrm{th}}}{M_e^{\mathrm{th}}}\right]^{1/2} . \tag{7}$$

The output voltage V of the NMR laser, which is proportional to M_v, fulfills, therefore, a power law with the critical exponent $\beta = \frac{1}{2}$. In Fig. 4 we

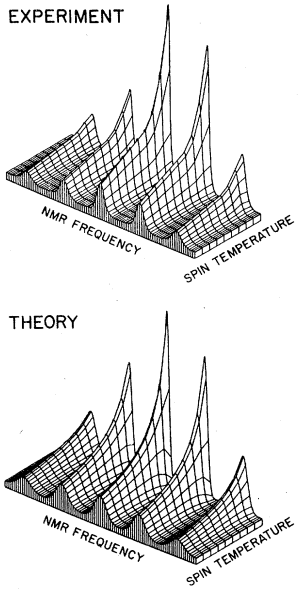

FIG. 3. Critical narrowing of the NMR resonance lines of ^{27}Al vs the pumping power or the nuclear spin temperature.

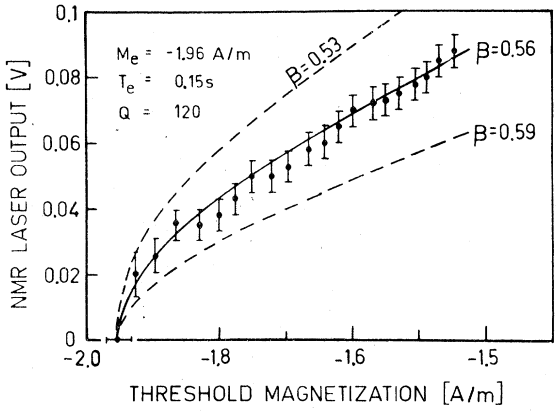

FIG. 4. NMR laser output voltage vs the threshold magnetization M_e^{th} with the three fits for the critical Landau exponent $\beta = 0.53$, 0.56, 0.59. The best fit is obtained with $\beta = 0.56$.

have plotted experimental values V^s vs M_e^{th} together with various fits in accord with (7). For experimental reasons M_e was kept constant, while M_e^{th} was varied by imposing a small field gradient to the static field, thus changing T_2. The pumping magnetization M_e was determined by measuring the spin temperature of the ^{27}Al spin system in the pumped state. The best fit is reached with $\beta_{exp} = 0.56$. The discrepancy between theory and experiment is not yet understood but could be found either in the inhomogeneous broadening caused by the field gradient, or in the fact that M_e is a weak function of the power output rather than a constant as assumed.

To demonstrate the close correspondence between this disorder-order transition far from thermal equilibrium with Landau-type second-order phase transitions at thermal equilibrium, we introduce in analogy to the free energy a NMR laser potential[1]

$$\Phi = \tfrac{1}{2}\alpha M_v^2 + \tfrac{1}{4}\epsilon M_v^4 , \tag{8}$$

such that (5a) can be written as

$$\dot{M}_v = -\frac{\partial \Phi}{\partial M_v} + \tilde{F}_B(t) . \tag{9}$$

We follow Haken[1] further and define the NMR laser entropy or NMR laser action S together with the specific NMR laser action C such that

$$S = -\frac{\partial \Phi}{\partial M e} , \tag{10}$$

$$C = -M_e \frac{\partial^2 \Phi}{\partial M_e^2} . \tag{11}$$

For $\alpha < 0$ we find $S = (M_e - M_e^{th})/2T_e$ if we set $S = 0$ for $\alpha > 0$.

Numerical values of $M_v(M_e)$, $\Phi(M_e)$, $S(M_e)$, and $C(M_e)$ for our system are depicted in Fig. 5 together with the steady-state solution (7) for the order parameter M_v.

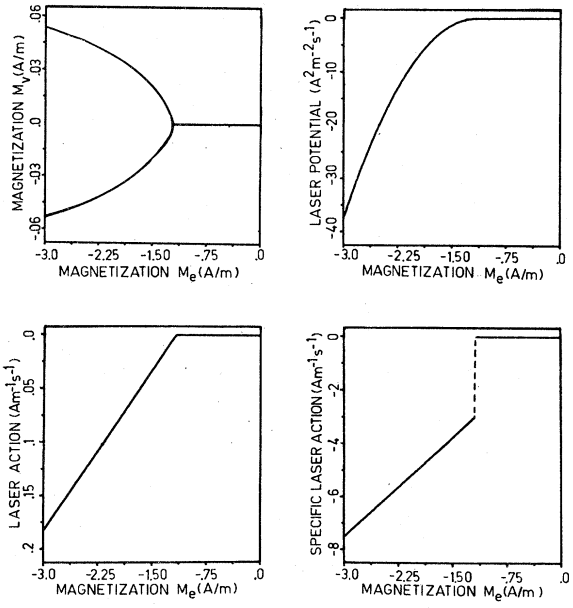

FIG. 5. Steady-state magnetization M_v, potential Φ, NMR laser action (entropy) $-d\Phi/M_e$, and specific NMR laser action (specific heat) $-M_e(d^2\Phi/dM_e^2)$ vs the pump magnetization M_e. The NMR laser action is continuous at the critical point; the phase transition is of second order.

IV. rf-DRIVEN NMR LASER

Consider the same NMR laser system as in Sec. III but place the sample in an external rf field which has the properly rotating component B_1^{ex} such that sign $(B_1^{ind}) = -$sign (B_1^{ex}) or sign $(B_1^{ind}) = +$sign(B_1^{ex}). The plus sign indicates the cooperative field configuration $B_1^{ex} \uparrow\uparrow B_1^{ind}$, the minus sign the competitive one $B_1^{ex} \uparrow\downarrow B_1^{ind}$. Equation (1c) reads now

$$B_1 = B_1^{ind} + B_1^{ex} + F_B(t) , \tag{12}$$

with

$$B_1^{ind} = -\tfrac{1}{2}\mu_0 \eta Q M_v , \tag{13}$$

whereas elimination of B_1 in (1a) and (1b) leads to the new dynamic equations

$$\dot{M}_v = (-\tfrac{9}{2}\mu_0 \eta Q \gamma M_v + 9\gamma B_1^{ex}) M_z - M_v/T_2 , \tag{14a}$$

$$\dot{M}_z = \tfrac{1}{2}\mu_0 \eta Q \gamma M_v^2 - \gamma B_1^{ex} M_v - (M_z - M_e)/T_e , \tag{14b}$$

if the fluctuations are neglected.

In order to treat the NMR laser dynamics near the steady states, we introduce again the NMR laser potential

$$\Phi = \rho M_v + \tfrac{1}{2}\alpha M_v^2 + \tfrac{1}{3}\delta M_v^3 + \tfrac{1}{4}\epsilon M_v^4 , \tag{15a}$$

with

$$\rho = -9\gamma B_1^{ex} M_e , \tag{15b}$$

$$\alpha = \tfrac{9}{2}\mu_0 \eta Q \gamma M_e + 9\gamma^2 (B_1^{ex})^2 T_e + 1/T_2 , \tag{15c}$$

$$\delta = -9\mu_0 \eta Q \gamma^2 B_1^{ex} T_e , \tag{15d}$$

$$\epsilon = \tfrac{9}{4}\mu_0^2 \eta^2 Q^2 \gamma^2 T_e , \tag{15e}$$

from which we obtain the dynamic-order-parameter equation

$$\dot{M}_v = -\frac{\partial \Phi}{\partial M_v} + \tilde{F}_B(t) . \tag{16}$$

Figure 6 shows the potential of our system for different values of the pumping magnetization M_e and the external field B_1^{ex}. Each curve has a cooperative and a competitive branch. Neglecting the fluctuations, the stable steady-state solutions are functions of M_e and B_1^{ex}. They correspond to the

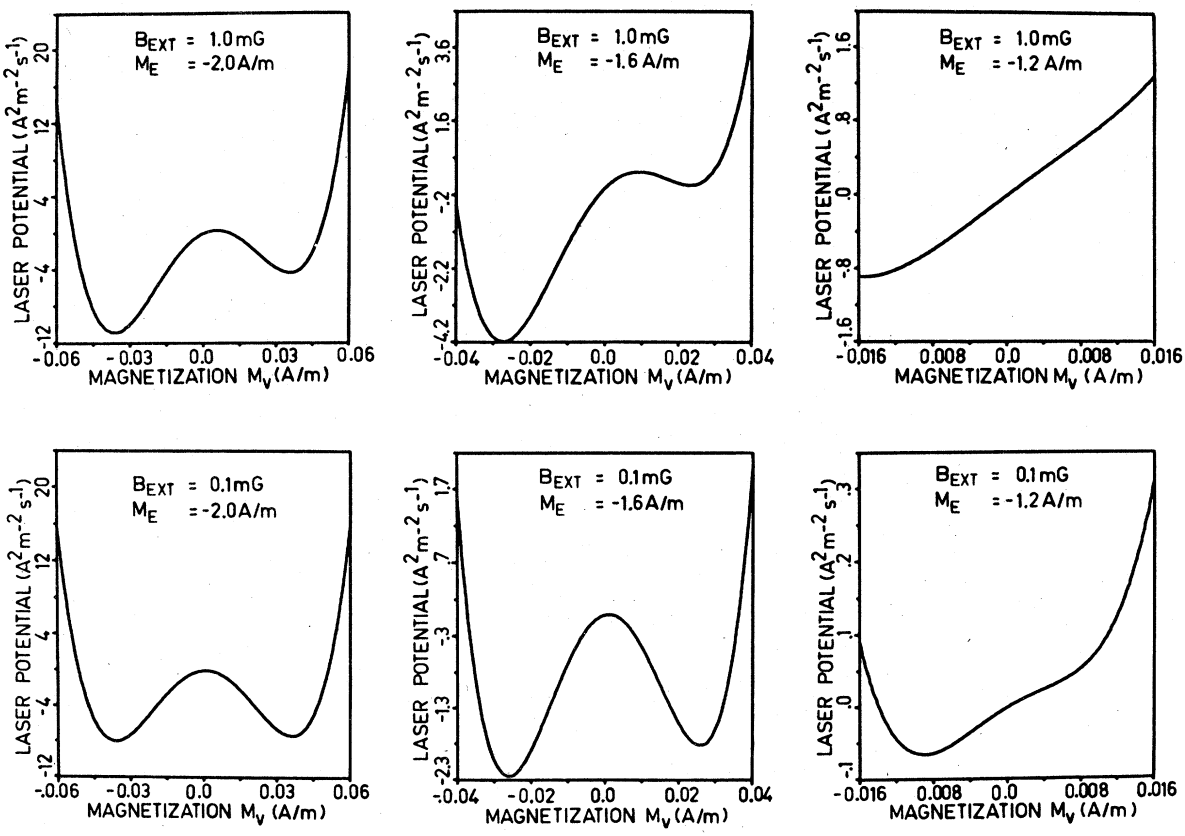

FIG. 6. Potential of the externally driven NMR laser vs M_v for different values of B_1^{ex} and M_e. The minima of the potentials correspond to the stationary solutions of (14). The minima with $B_1^{ind} \uparrow\uparrow B_1^{ex}$ (cooperative branch) are lower and therefore more stable than the ones with $B_1^{ind} \uparrow\downarrow B_1^{ex}$ (competitive branch).

minima of $\Phi(M_v)$. If both branches have a minimum then the one for $B_1^{ex}\uparrow\uparrow B_1^{ind}$ is lower (more stable) than the one for $B_1^{ex}\uparrow\downarrow B_1{}^{ind}$. With increasing absolute magnitude of B_1^{ex} the former solution remains stable; the latter one runs into an instability as soon as the external field reaches a critical value B_{1c}^{ex} in the competitive mode. When this occurs, the system must perform a transition to a stable mode. Making use of the bistability of this device, hysteresis loops, as depicted in Fig. 7, can be traced out which are typical for systems with a first-order phase transition. A similar behavior can be expected when M_e is changed while keeping B_1^{ex} constant. Starting from a stable state on the competitive branch and lowering the pumping power (thus increasing M_e), the system again reaches an instability as it is shown in Fig. 8. There the order parameter jumps irreversibly to a stable state on the cooperative branch. Additional insight into the nature of the instabilities can be gained by looking at the NMR laser action S and the specific NMR laser action C defined by Eqs. (10) and (11). The derivatives have to be taken at constant B_1^{ex} under steady-state conditions. Numerical values $S(M_e)$ and $C(M_e)$ together with $\Phi(M_e)$ are plotted in Fig. 9. Obviously, S and C are different for the two branches. In par-

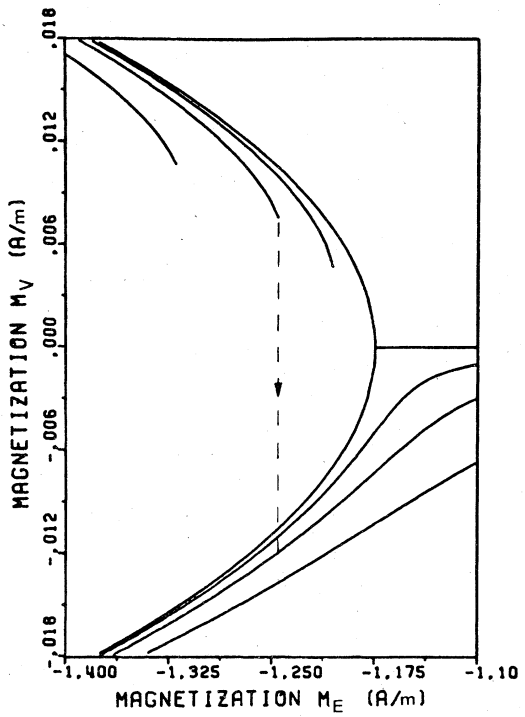

FIG. 8. Steady-state transverse magnetization M_v vs pump magnetization M_e for different values of B_1^{ex}. The dashed line indicates the transition at the instability point.

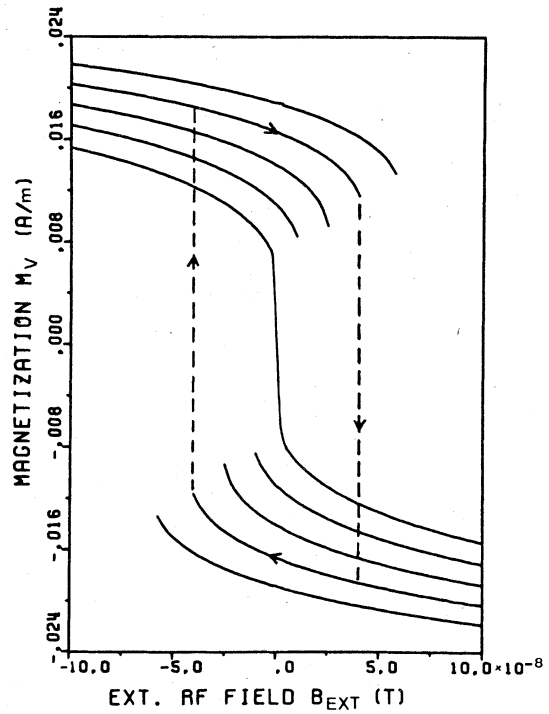

FIG. 7. Steady-state transverse magnetization M_v vs external driving rf field B_1^{ex} for different values of M_e. The arrows indicate one of the possible hysteresis loops.

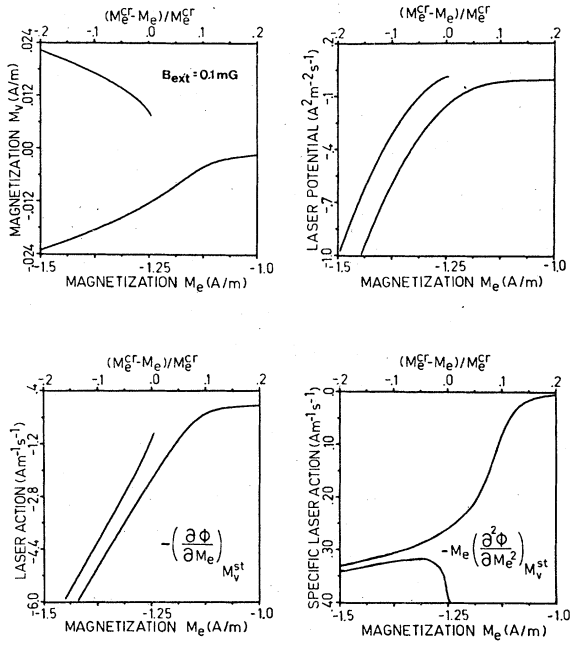

FIG. 9. Steady-state magnetization M_v, potential Φ, action (entropy) $-d\Phi/dM_e$, and specific action (specific heat) $-M_e(d^2\Phi/dM_e^2)$ vs pump magnetization M_e for the NMR laser driven with a resonant external rf field. The NMR laser action is discontinuous at the critical point; the phase transition is of first order.

ticular, S becomes discontinuous at the instability point on the competitive branch. The subsequent transition for a stable state is, as indicated before, a first-order-type phase transition.

In order to observe these first-order transitions directly, we investigated, both experimentally and theoretically, the transient response of the initially free-running NMR laser when an external rf field is abruptly turned on. The dynamic equation (16) is not adequate to handle such a situation. In this case the full dynamics of the reservoir model[3] has to be put into Eqs. (12) and (14) to calculate the nonlinear response of the system. Here we describe three special cases.

In all three experiments, the NMR laser is brought initially to a free-running steady-state mode. First, we switch on a competitive field such that B_1^{ex} is smaller than the critical value B_{1c}^{ex}. The output shows a transient signal in the form of a damped relaxation oscillation. The NMR laser reaches a new stable state on the competitive branch within a fraction of a second. This is demonstrated experimentally and theoretically in Fig. 10. Next, we switch on a competitive field such that B_1^{ex} is larger than the critical field B_{1c}^{ex}. The NMR laser output shows, in a first phase, an exponentially growing amplitude-modulated transient until B_1^{ex} and B_1^{ind} cancel. At this moment the NMR laser action is small. Due to the lack of a strong slaving field, the nuclear spins have a chance to lose their phase memory with respect to the initial state. From there on they begin to precess cooperatively with B_1^{ex}. Hence, a field B_1^{ind} is induced with $B_1^{ex} \uparrow\uparrow B_1^{ind}$. Thus, in the second phase of the transient, an amplitude-modulated relaxation oscillation is observed which, finally, evolves into a new stable state on the cooperative branch. The system has thus performed a first-order-type phase transition. The experimental and calculated response is shown in Fig. 11. Note that B_1^{ex} is some orders of magnitude smaller than B_1^{ind} in the free-running mode.

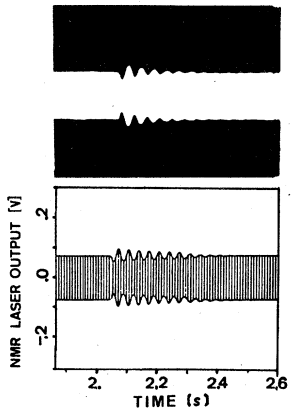

FIG. 10. Response of the free-running NMR laser after turning on an external, competitive rf field $B_1^{ex} < B_{1c}^{ex}$.

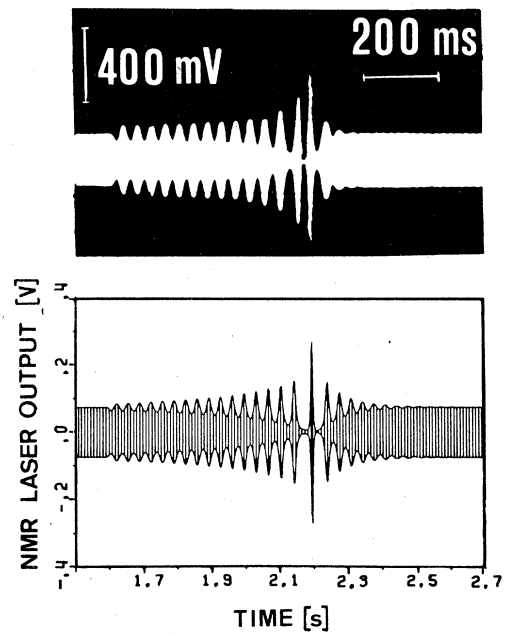

FIG. 11. Response of the free-running NMR laser after turning on an external, competitive rf field $B_1^{ex} > B_{1c}^{ex}$.

In a third experiment, we switch on a competitive field $B_1^{ex} > B_{1c}^{ex}$ which, by means of an electronic control, is always kept in the competitive configuration $B_1^{ex} \uparrow\downarrow B_1^{ind}$. Again, the system responds with an exponentially growing amplitude-modulated

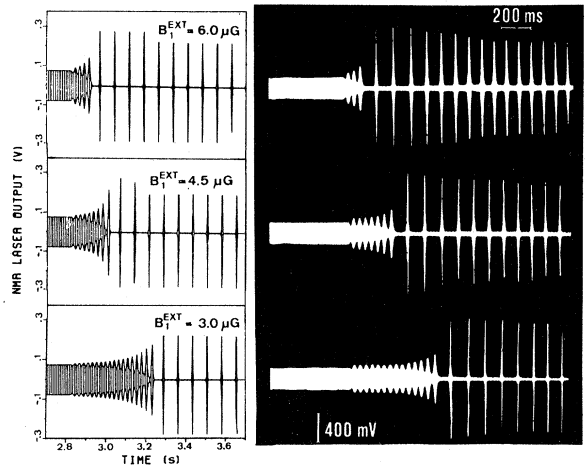

FIG. 12. Response of the free-running NMR laser after turning on an external, competitive rf field $B_1^{ex} > B_{1c}^{ex}$. By electronic means, the competitive field configuration is maintained in the subsequent unsteady NMR laser action.

oscillation until the NMR laser action ceases. From there on, as a consequence of the interplay between pumping, cooperative self-ordering, and external field in a competitive state, the NMR laser emits a regular train of superradiant bursts such that one is tempted to call this system a NMR pulsar. Figure 12 shows experimental and theoretical response curves for different values of B_1^{ex}.

V. CONCLUDING REMARKS

The dynamical aspect of the ruby NMR laser have been discussed from the point of view of synergetics. The instabilities and spontaneous transitions from nonradiating to radiating states or from one particular radiating to another radiating state of a negatively polarized nuclear-spin system have their analogue in systems with conventional second- or first-order phase transitions. The good agreement between the theoretical Bloch-equation approach and the experiments stems from the fact that we have considered only the purely absorptive response under exact resonance conditions. Dispersion, however, becomes of importance in detuned systems. In particular, when the NMR laser is driven with a nonresonant rf field, beat patterns appear which are rich in their forms. However, a systematic investigation of the dispersive features, both theoretically and experimentally, remains to be done.

ACKNOWLEDGMENTS

We wish to thank Professor Redfield for the stimulating correspondence that has been very helpful in this work. We also want to thank Professor K. V. Vladimirsky and Dr. P. Meier for interesting discussions. Finally, we wish to express our gratitude to the Swiss National Science Foundation (Schweiz. Nationalfonds) for the financial support.

[1]H. Haken, *Synergetics* (Springer, Berlin, 1977).
[2]P. Bösiger, E. Brun, and D. Meier, Phys. Rev. Lett. 38, 602 (1977).
[3]P. Bösiger, E. Brun, and D. Meier, Phys. Rev. A 18, 671 (1978).
[4]N. Bloembergen and R. V. Pound, Phys. Rev. 95, 8 (1954).
[5]K. V. Vladimirsky, Nucl. Instrum. 1, 399 (1957).
[6]S. Bloom, J. Appl. Phys. 28, 800 (1957).
[7]A. Szöke and S. Meiboom, Phys. Rev. 113, 585 (1959).
[8]P. Bösiger, E. Brun, and D. Meier, in Proceedings of the 20th Congress Ampere, Tallinn, 1978 (North-Holland, Amsterdam, in press).
[9]P. Bösiger, E. Brun, and D. Meier, Proceedings of the Fourth General Conference of the European Physical Society, York, 1978, in Trends of Physics (Institute of Physics, London, in press).
[10]H. M. Gibbs, S. L. McCall, and T. N. C. Venkatesan, Phys. Rev. Lett. 36, 1135 (1976).
[11]R. Bonifacio and L. A. Lugiato, Opt. Commun. 19, 172 (1976).
[12]H. J. Carmichael and D. F. Walls, J. Phys. B 9, 1 (1977).
[13]G. S. Agarwal, L. M. Narducci, R. Gilmore, and Da Hsuan Feng, Phys. Rev. A 18, 620 (1978).
[14]A. Abragam, J. Combrisson, and I. Solomon, C. R. Acad. Sci. 245, 157 (1957).
[15]H. Haken, in *Handbuch d. Physik*, edited by S. Flügge (Springer, Berlin, 1970), p. 186.
[16]F. Bloch, Phys. Rev. 70, (1946).
[17]A. G. Redfield, Phys. Rev. 98, 1787 (1955).

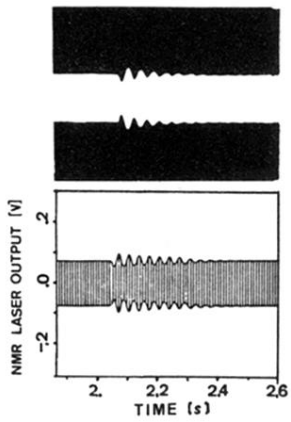

FIG. 10. Response of the free-running NMR laser after turning on an external, competitive rf field $B_1^{ex} < B_{1c}^{ex}$.

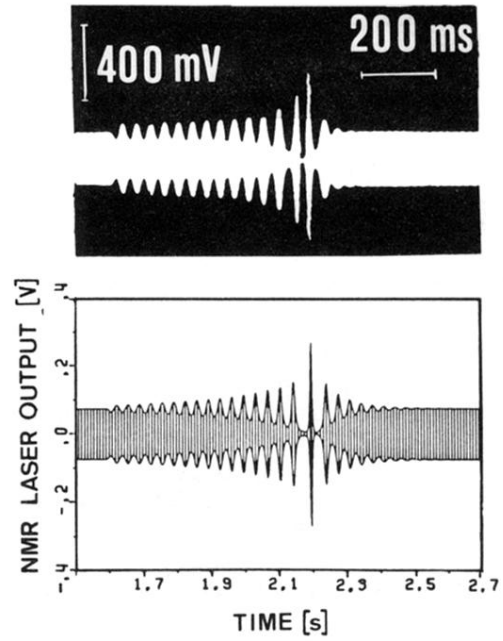

FIG. 11. Response of the free-running NMR laser after turning on an external, competitive rf field $B_1^{ex} > B_{1c}^{ex}$.

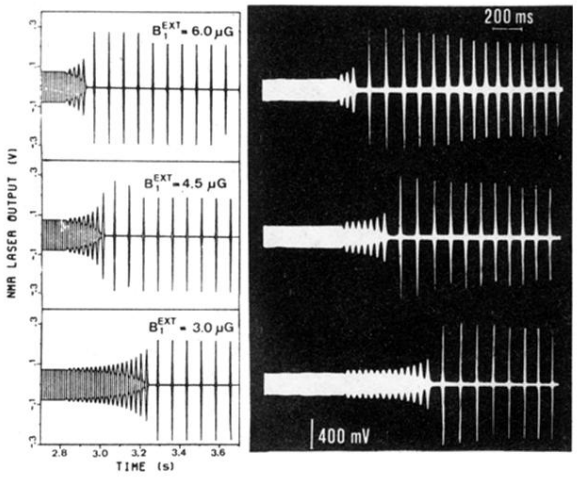

FIG. 12. Response of the free-running NMR laser after turning on an external, competitive rf field $B_1^{ex} > B_{1c}^{ex}$. By electronic means, the competitive field configuration is maintained in the subsequent unsteady NMR laser action.